

## Supporting Information

# In situ synthesis of ordered mesoporous Co-doped TiO<sub>2</sub> and their enhanced photocatalytic activities and selectivities in reduction of CO<sub>2</sub>

*Tao Wang<sup>1</sup>, Xianguang Meng<sup>1,2</sup>, Guigao Liu<sup>1,2</sup>, Kun Chang<sup>1</sup>, Peng Li<sup>1</sup>, Qing Kang<sup>1</sup>,  
Lequan Liu<sup>1,3,4</sup>, Mu Li<sup>1,2</sup>, Shuxin Ouyang<sup>3,4</sup>, and Jinhua Ye<sup>1,2,3,4\*</sup>*

<sup>1</sup>International Center for Materials Nanoarchitectonics (WPI-MANA), and Environmental Remediation Materials Unit, National Institute for Materials Science (NIMS), 1-1 Namiki, Tsukuba, Ibaraki, 305-0044, Japan

<sup>2</sup>Graduate School of Chemical Science and Engineering, Hokkaido University, Sapporo, 060-0814, Japan

<sup>3</sup>TU-NIMS Joint Research Center, School of Materials Science and Engineering, Tianjin University, 92 Weijin Road, Tianjin, 300072, P.R. China

<sup>4</sup>Collaborative Innovation Center of Chemical Science and Engineering (Tianjin), Tianjin, 300072, P.R. China.

\* To whom correspondence should be addressed: E-mail: [Jinhua.YE@nims.go.jp](mailto:Jinhua.YE@nims.go.jp)

## **Additional experimental section:**

### **1 Synthesis of reference samples**

For purposes of comparison in the same reactor system, we synthesize or buy some typical semiconductors or composites, including Degussa P-25, N-doped TiO<sub>2</sub>, Au/TiO<sub>2</sub>, C<sub>3</sub>N<sub>4</sub>, WO<sub>3</sub>). The performance and characteristics of these materials are shown in Fig. S8 and Table S2. Degussa P-25(TiO<sub>2</sub>) was bought from Evonik-Degussa; ST-01(TiO<sub>2</sub>) and WO<sub>3</sub> were bought from Wako pure chemical industries.

Synthesis of N-doped TiO<sub>2</sub>: in a typical preparation, a certain amount of ST-01 was annealed in a tubular furnace at 550 °C for 2 h under NH<sub>3</sub> atmosphere. The sample was named as N-TiO<sub>2</sub>.

Synthesis of Au/TiO<sub>2</sub>: in a typical preparation, ordered mesoporous TiO<sub>2</sub> (OMT) powder was immersed into a certain amount of HAuCl<sub>4</sub> aqueous solution. Then, a small amount of ascorbic acid aqueous solution was added to reduce Au. The theoretical weight percentage of Au is about 7%. The sample was named as Au-OMT.

Synthesis of bulk g-C<sub>3</sub>N<sub>4</sub>: in a typical preparation,<sup>R1</sup> a certain amount of dicyandiamide was annealed in a tubular furnace at 550 °C for 4 h under air atmosphere.

## 2 Calculation of the quantum efficiency

On the basis of the assumption that a photon must be effectively absorbed, the photocatalytic quantum efficiency (QE) is typically defined as the ratio of the rate of photocatalytic events to the absorbed photons.<sup>R2,R3</sup>

$$QE = \frac{N_{\text{photocat. events}}}{N_{\text{absorbed photons}}}$$

The photocatalytic events have to be summed over the (molar) amounts of all the products,  $N_{\text{photocat. events}} = \sum_i n_i M_i$ , Where  $n_i$  is the number of electrons required to obtain one molecule of product  $M_i$ .

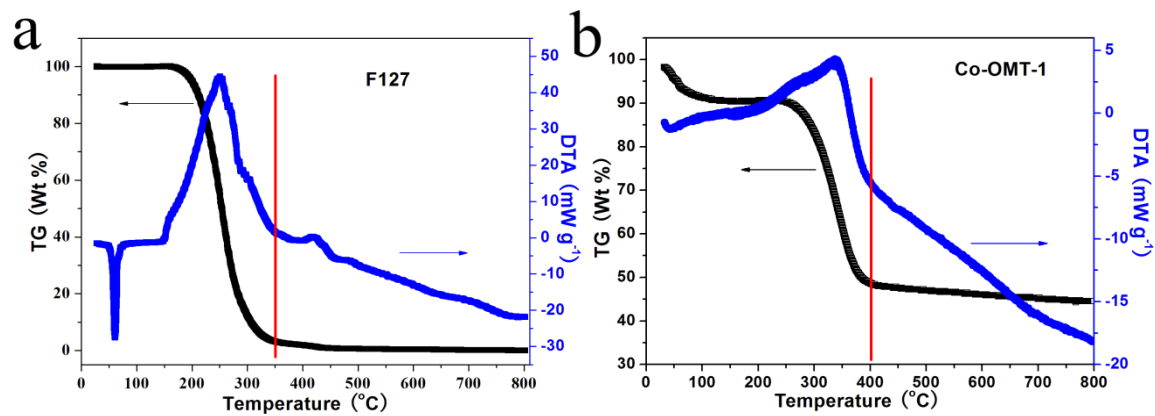


**Fig. S1** TG/DTA curves of F127 (a) recorded in N<sub>2</sub> and Co-OMT-1 (b) recorded in air

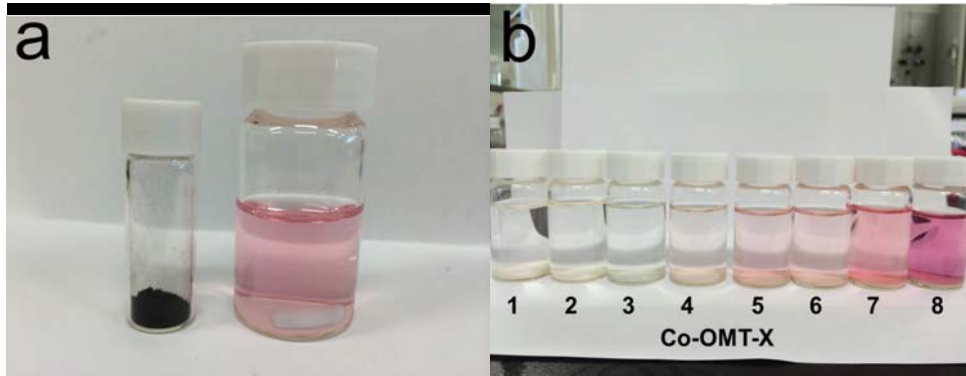


**Fig. S2** (a) The photo of of  $\text{Co}_3\text{O}_4$  before and after dissolving by HCl. (b) The photos of Co-doped  $\text{TiO}_2$  dissolving by HCl to remove the  $\text{Co}_3\text{O}_4$ .

**Table S1** The molar ratio of samples before and after removing the  $\text{Co}_3\text{O}_4$ .

Sample	Theoretical molar ratio (Co: Ti) <sup>[a]</sup>	Practical molar ratio (Co: Ti) <sup>[b]</sup>	Doping levels of $\text{Co}^{2+}$ (Co: Ti) <sup>[c]</sup>
OMT	0	0	0
Co-OMT-1	0.002	0.0023	0.0020
Co-OMT-2	0.005	0.0049	0.0021
Co-OMT-3	0.01	0.013	0.0040
Co-OMT-4	0.025	0.026	0.0041
Co-OMT-5	0.05	0.053	0.0049
Co-OMT-6	0.1	0.12	0.0063
Co-OMT-7	0.15	0.15	0.0064
Co-OMT-8	0.2	0.25	0.0045
$\text{Co}_3\text{O}_4$	-	-	-

[a] The value is calculated according to the additive amount in the synthetic process.

[b] The value is calculated according to the EDX analysis before removing the  $\text{Co}_3\text{O}_4$ .

[c] The value is calculated according to the EDX analysis after removing the  $\text{Co}_3\text{O}_4$ .

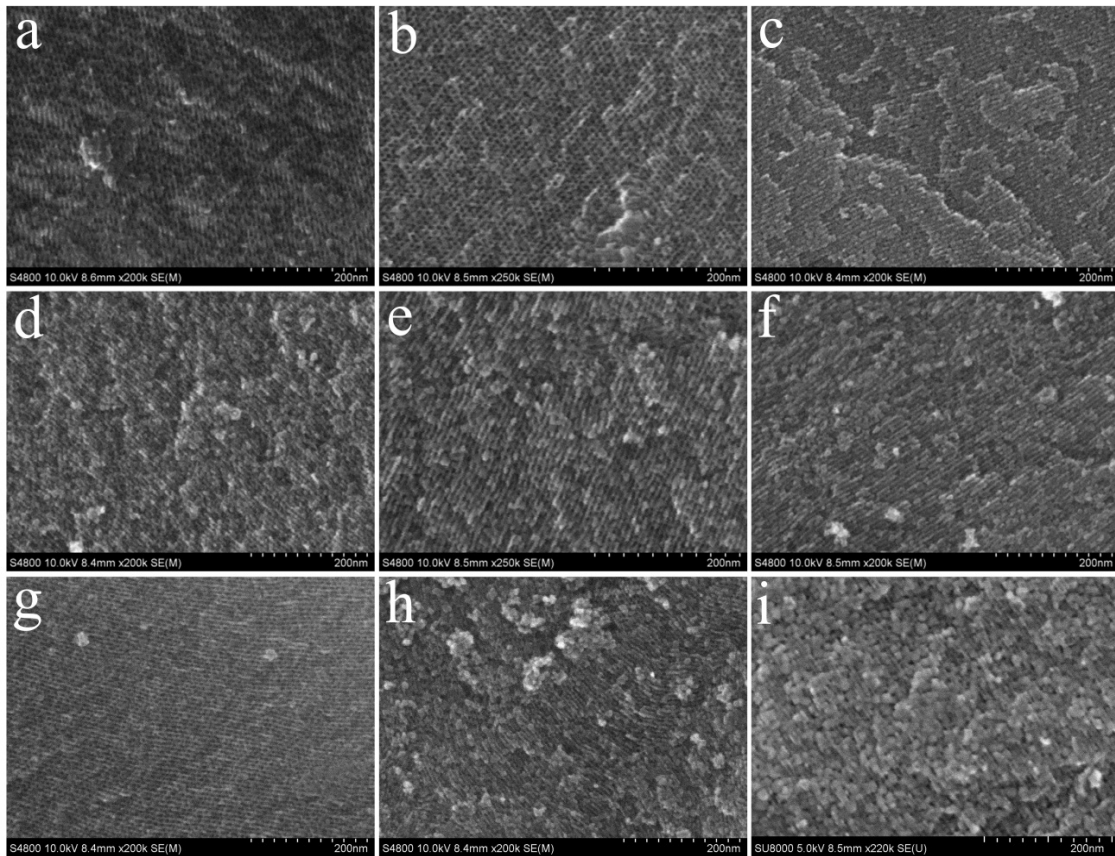


**Fig. S3** FE-SEM images of samples: (a) OMT, (b) Co-OMT-1, (c) Co-OMT-2, (d) Co-OMT-3, (e) Co-OMT-4, (f) Co-OMT-5, (g) Co-OMT-6, (h) Co-OMT-7, (i) Co-OMT-8.

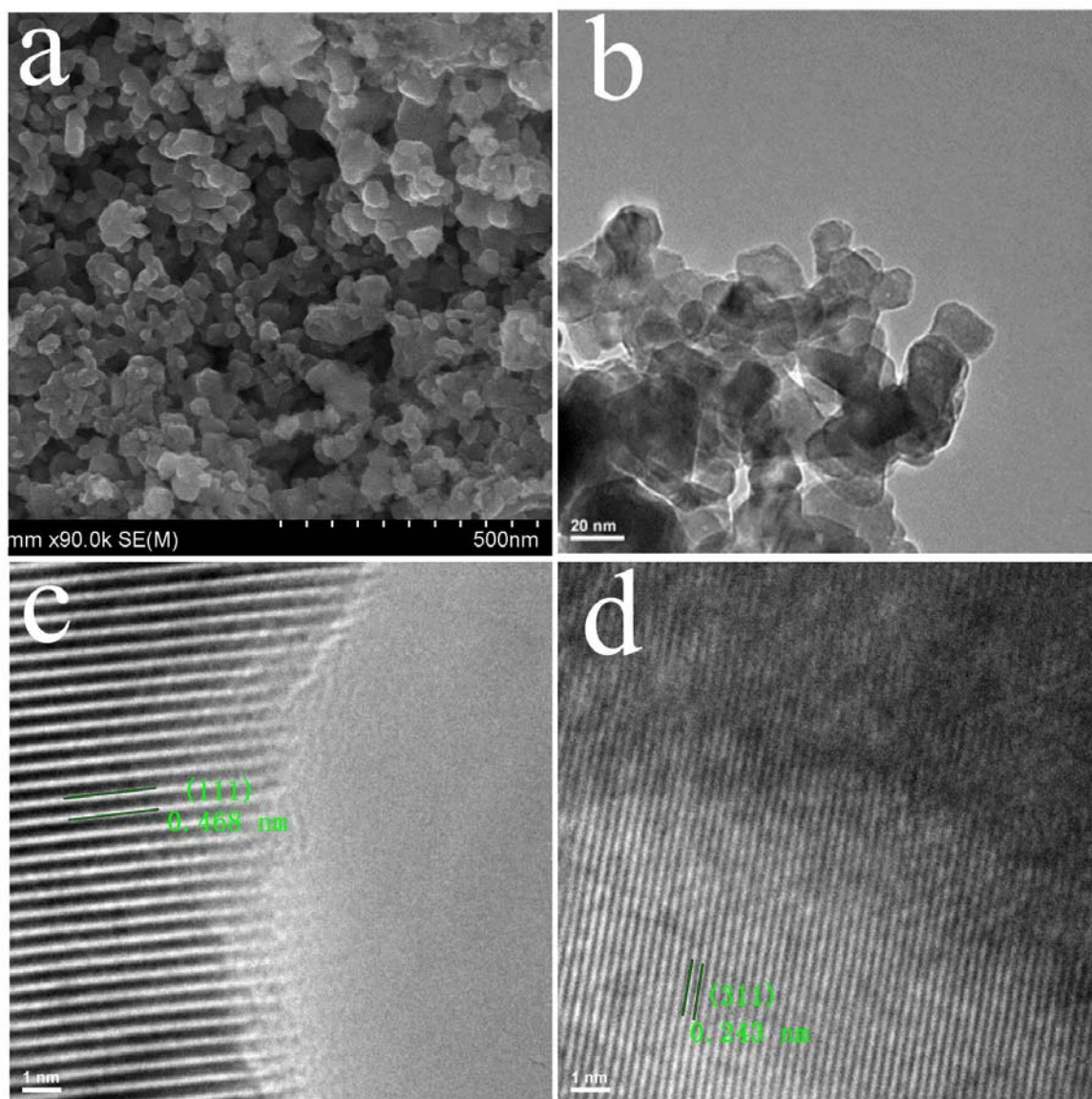


**Fig. S4** (a) FE-SEM and (b,c,d) TEM images of  $\text{Co}_3\text{O}_4$ .

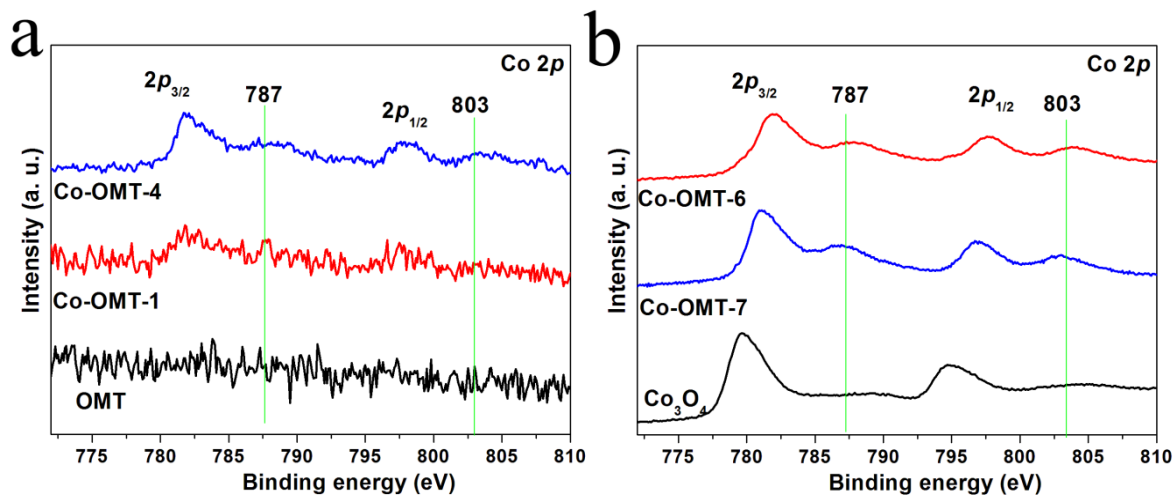
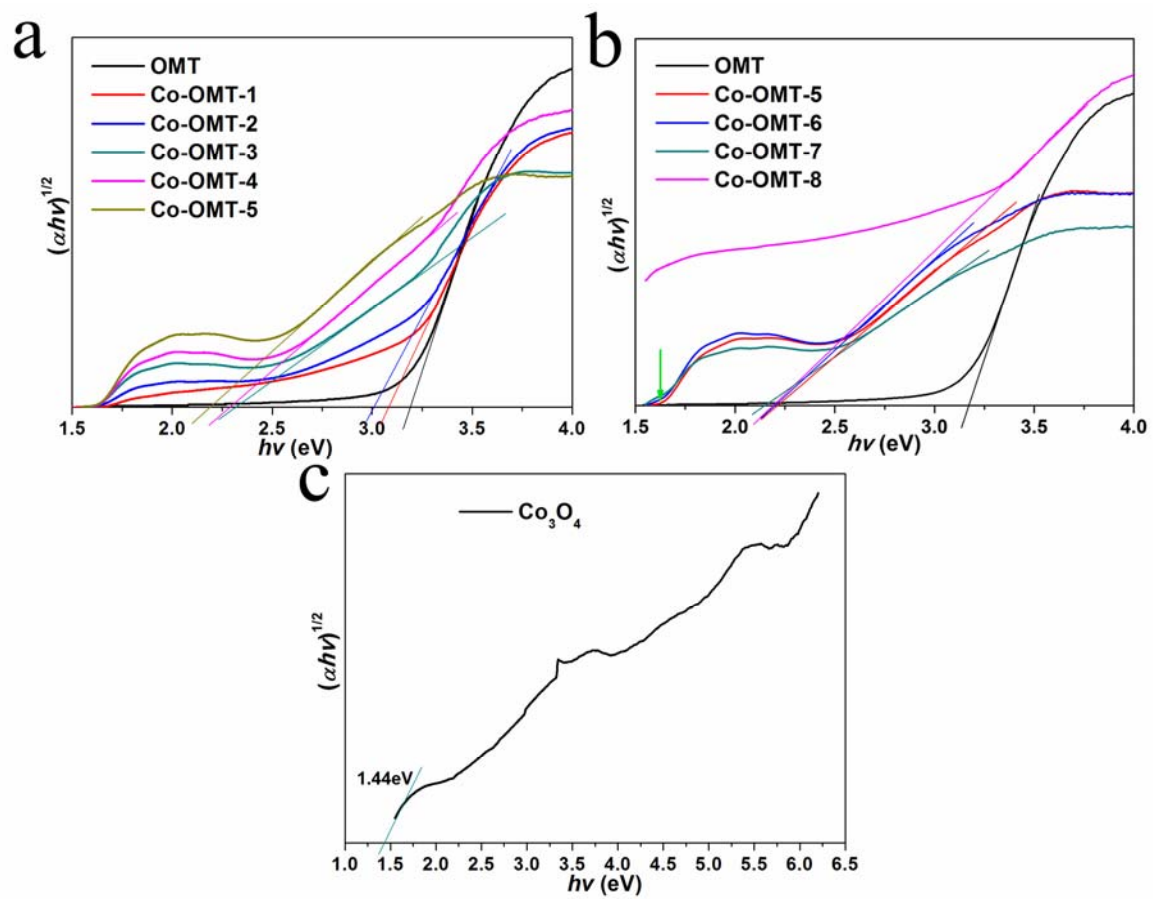
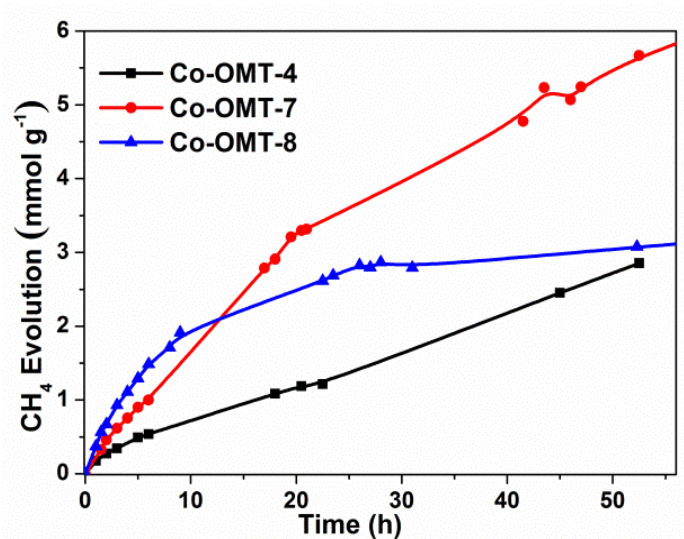


Fig. S5 X-ray photoelectron spectroscopy of samples.





**Fig. S6** The Tauc plots of samples.



**Fig. S7** CH<sub>4</sub> evolution over Co-OMT-4, Co-OMT-7 and Co-OMT-8 under visible light.

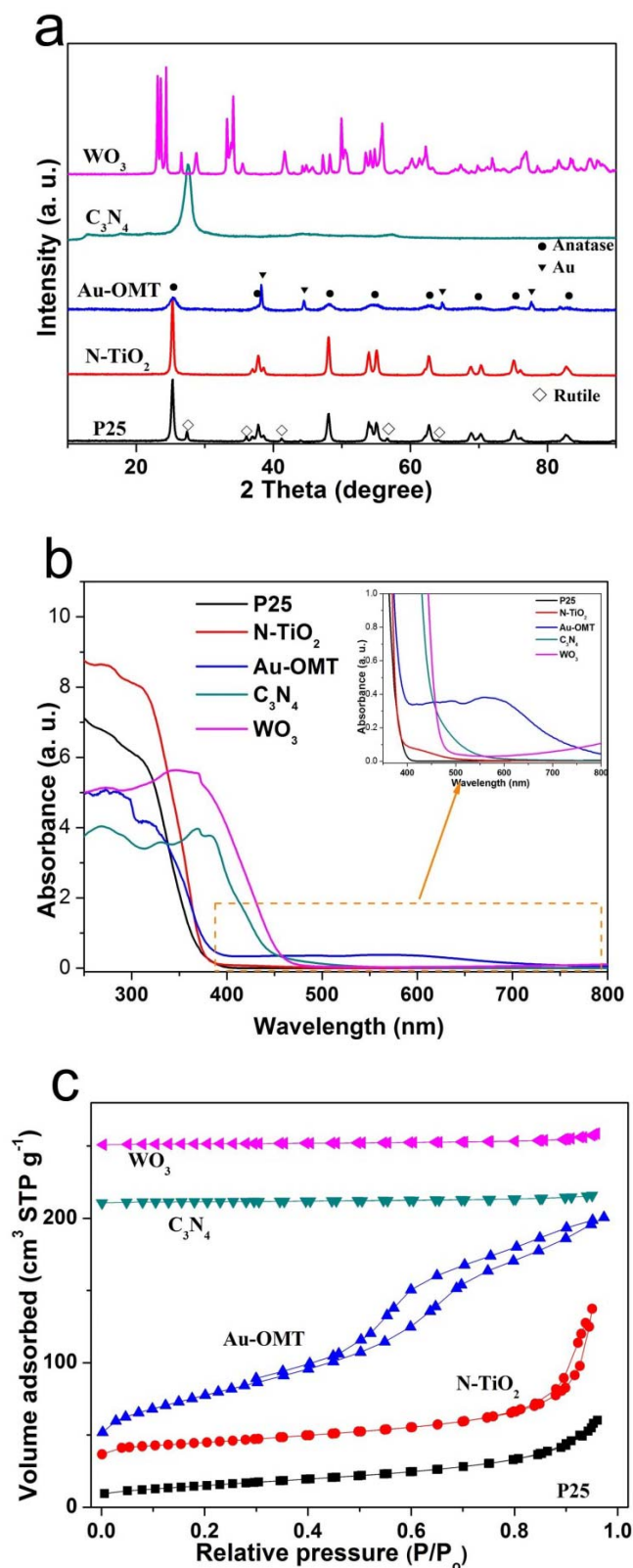


**Fig. S8** (a) Wide-angle XRD patterns, (b) UV-vis absorption spectra and (c) N<sub>2</sub> adsorption-desorption isotherms of samples.

The wide-angle XRD patterns of samples were shown in Fig. S8a. We can see that P25 presents a mixture of anatase and rutile; N-TiO<sub>2</sub> presents anatase; Au-OMT

presents a mixture of anatase and gold. The characteristic peaks of C<sub>3</sub>N<sub>4</sub> are same as the previous reports.<sup>R1</sup> UV-visible absorption spectra (Fig. S8b) show that all samples except P25, possess the optical absorption capability in the visible light region. The specific surface areas of P25, N-TiO<sub>2</sub>, Au-OMT, C<sub>3</sub>N<sub>4</sub>, WO<sub>3</sub> were 54.4, 53.6, 181.0, 5.2, 5.4 m<sup>2</sup> g<sup>-1</sup>, respectively (calculated by the BET method from N<sub>2</sub> adsorption-desorption isotherms in Figure S8c).

**Table S2** Summary of the various photocatalytic systems employed for CO<sub>2</sub> reduction.

Catalyst	Co-catalyst	Light source	Conditions	Major products	R <sub>max</sub> <sup>[a]</sup>	Ref.
Co-OMT-4	-	Visible light: 300 W Xe lamp with a cut-off filter ( $\lambda > 420$ nm)	CO <sub>2</sub> and H <sub>2</sub> O vapor	CH <sub>4</sub> CO	0.09 1.94	This study
		UV-Vis light: 300 W Xe lamp	CO <sub>2</sub> and H <sub>2</sub> O vapor	CH <sub>4</sub> CO	0.33 2.09	This study
P25	-	Visible light: 300 W Xe lamp with a cut-off filter ( $\lambda > 420$ nm)	CO <sub>2</sub> and H <sub>2</sub> O vapor	None	0	This study
N-TiO <sub>2</sub>	-	Visible light: 300 W Xe lamp with a cut-off filter ( $\lambda > 420$ nm)	CO <sub>2</sub> and H <sub>2</sub> O vapor	CH <sub>4</sub> CO	0.015 0.153	This study
Au-OMT	-	Visible light: 300 W Xe lamp with a cut-off filter ( $\lambda > 420$ nm)	CO <sub>2</sub> and H <sub>2</sub> O vapor	CH <sub>4</sub> CO	0.018 0.056	This study
C <sub>3</sub> N <sub>4</sub>	-	Visible light: 300 W Xe lamp with a cut-off filter ( $\lambda > 420$ nm)	CO <sub>2</sub> and H <sub>2</sub> O vapor	CH <sub>4</sub> CO	0.031 0.135	This study
WO <sub>3</sub>	-	Visible light: 300 W Xe lamp with a cut-off filter ( $\lambda > 420$ nm)	CO <sub>2</sub> and H <sub>2</sub> O vapor	CH <sub>4</sub> CO	0.005 0.017	This study
ZnAl <sub>2</sub> O <sub>4</sub> -modified mesoporous ZnGaNO	0.5 wt% Pt	Visible light: 300 W Xe lamp with a cut-off filter ( $\lambda > 420$ nm)	CO <sub>2</sub> and H <sub>2</sub> O vapor	CH <sub>4</sub>	0.0092	R4
RGO–CdS nanorod composite	-	Visible light: 300 W Xe arc lamp with a cut-off filter ( $\lambda > 420$ nm)	CO <sub>2</sub> and H <sub>2</sub> O vapor	CH <sub>4</sub>	2.51	R5
P25	-	UV-Vis light: 300 W Xe lamp	CO <sub>2</sub> and H <sub>2</sub> O vapor	CH <sub>4</sub>	0.0027	R6
Ordered	-	UV-Vis light: 300 W	CO <sub>2</sub> and H <sub>2</sub> O	CH <sub>4</sub>	0.19	R6

mesoporous TiO <sub>2</sub>		Xe lamp	vapor	CO	0.15	
Zn <sub>2</sub> GeO <sub>4</sub> nanobelt	1 wt % Pt and 1 wt % RuO <sub>2</sub>	<b>UV-Vis light:</b> 300 W Xe lamp	CO <sub>2</sub> and H <sub>2</sub> O vapor	CH <sub>4</sub>	0.025	R7
Anatase TiO <sub>2</sub> rods with {010} facets	1 wt% Pt	<b>UV-Vis light:</b> 300 W Xe lamp	CO <sub>2</sub> and H <sub>2</sub> O vapor	CH <sub>4</sub>	0.0057	R8
Hollow anatase TiO <sub>2</sub> single crystals with {101} facets	1 wt% RuO <sub>2</sub>	<b>UV-Vis light:</b> 300 W Xe lamp	CO <sub>2</sub> and H <sub>2</sub> O vapor	CH <sub>4</sub>	0.0017	R9
Leaf-architected SrTiO <sub>3</sub>	1 wt % Au	<b>UV-Vis light:</b> 300 W Xe arc lamp	CO <sub>2</sub> and H <sub>2</sub> O vapor	CH <sub>4</sub> CO	0.28 0.35	R10
NaTaO <sub>3</sub>	1 wt % Au	<b>UV-Vis light:</b> 200 W Hg-Xe arc lamp	CO <sub>2</sub> and H <sub>2</sub> O vapor	CH <sub>4</sub> CO	0.036 0.17	R11
TiO <sub>2</sub> nanorod	Ag	<b>UV light:</b> four 8 W UVA lamps with a wavelength of 365 nm	CO <sub>2</sub> and H <sub>2</sub> O vapor	CH <sub>4</sub>	2.64	R12
Brookite TiO <sub>2</sub> nanorods	0.05 wt% Au	<b>UV light:</b> a light-emitting diode (Nichia, NCCU033), which emitted light at a wavelength of ca. 365 nm	5 mL of 0.2 mol L <sup>-1</sup> KHCO <sub>3</sub> aqueous solution saturated with CO <sub>2</sub>	CH <sub>3</sub> OH	0.11	R13
In-doped TiO <sub>2</sub>	-	<b>UV-vis light:</b> 500W mercury (Hg) flash lamp	CO <sub>2</sub> and H <sub>2</sub> O vapor, 0.20 bars reactor pressure, 373K reaction temperature	CH <sub>4</sub> CO	243.75 81.25	R14
MgO/TiO <sub>2</sub> nanotube film	Pt	<b>UV-vis light:</b> 300W high pressure Hg lamp	0.1 mol L <sup>-1</sup> KHCO <sub>3</sub> solution	CH <sub>4</sub>	100.22 <sup>[b]</sup>	R15

[a] Maximum formation rate reported for the major product(s), in  $\mu\text{mol g}^{-1}\text{h}^{-1}$ .

[b] In ppm h<sup>-1</sup> cm<sup>-1</sup>.

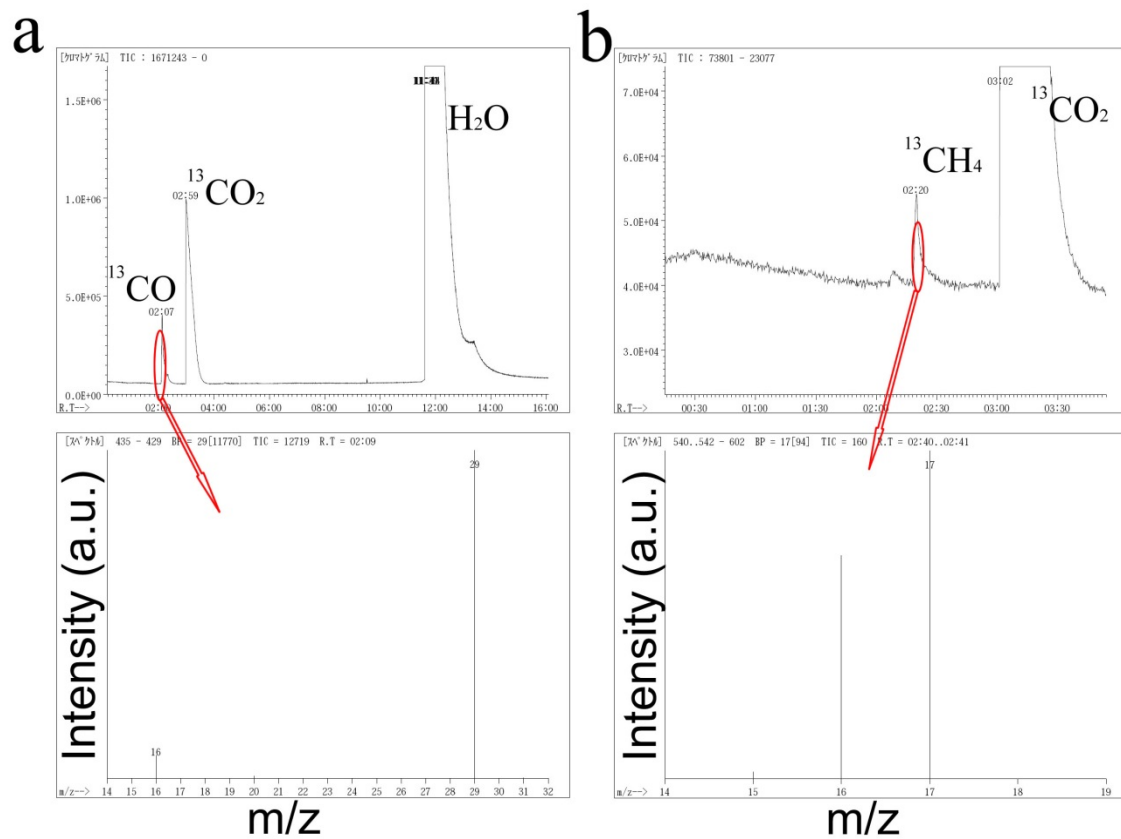


**Fig. S9** GC-MS spectra of the products of photocatalytic  $^{13}\text{CO}_2$  reduction over (a) Co-OMT-4 and (b) Co-OMT-7 after 12 h irradiation.

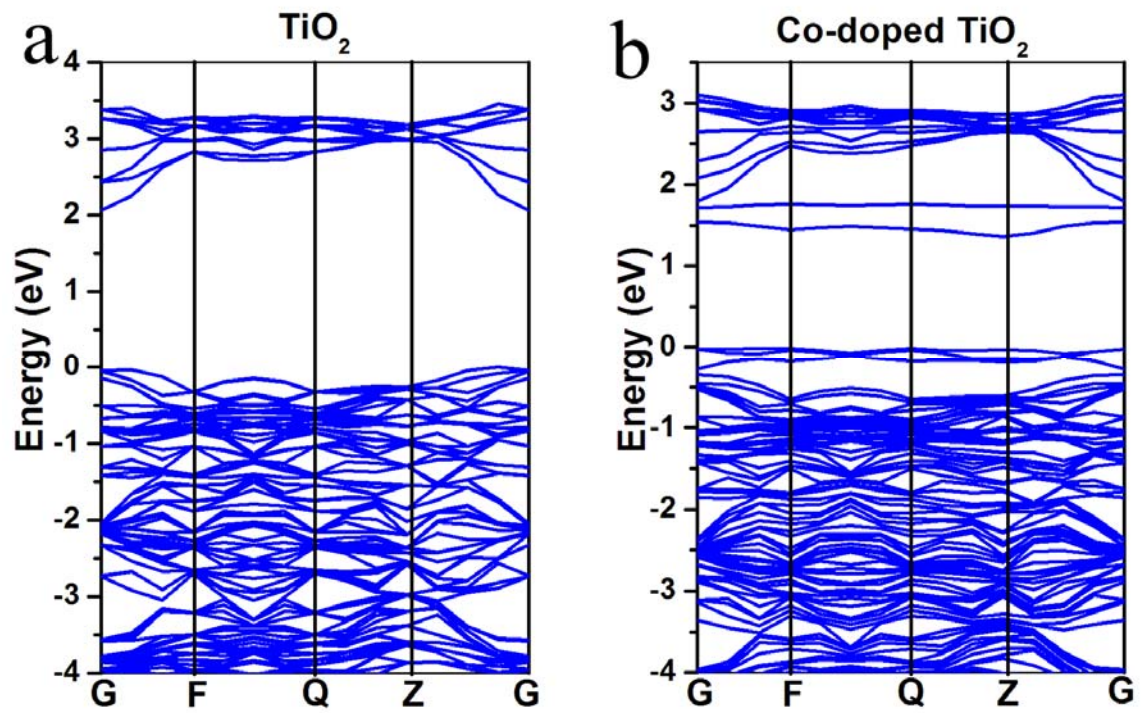


**Fig. S10** Electronic structures of (a) anatase  $\text{TiO}_2$  and (b)  $\text{Co}_x\text{Ti}_{1-x}\text{O}_2$  ( $x=0.0625$ ).

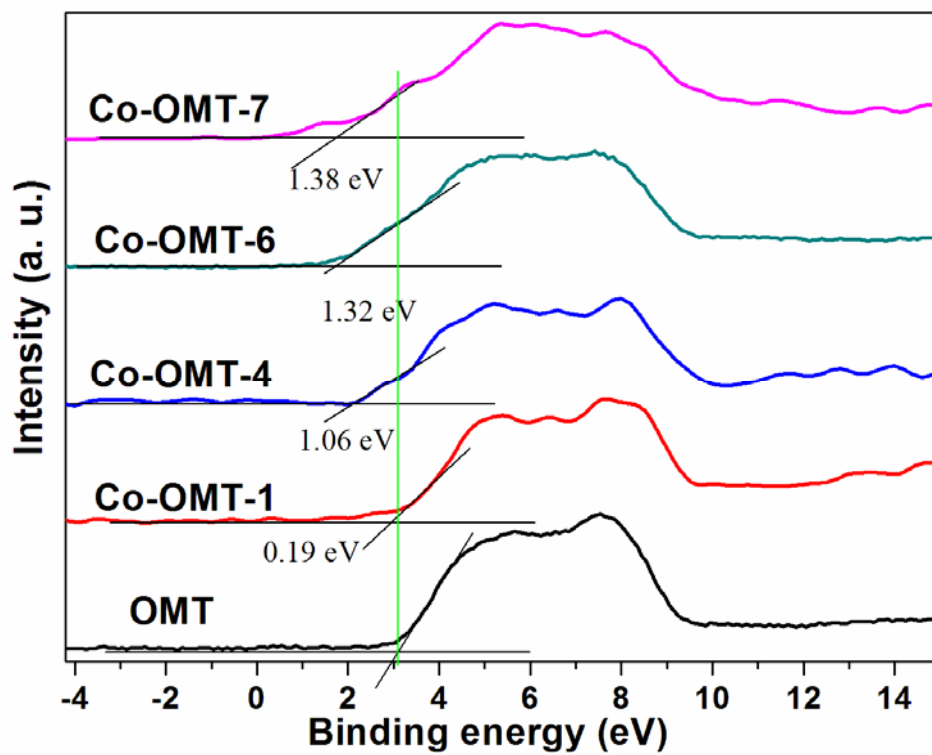


**Fig. S11** Valence band XPS spectra of samples. The values in Fig. are the relative difference between the Co-OMT-x and OMT.



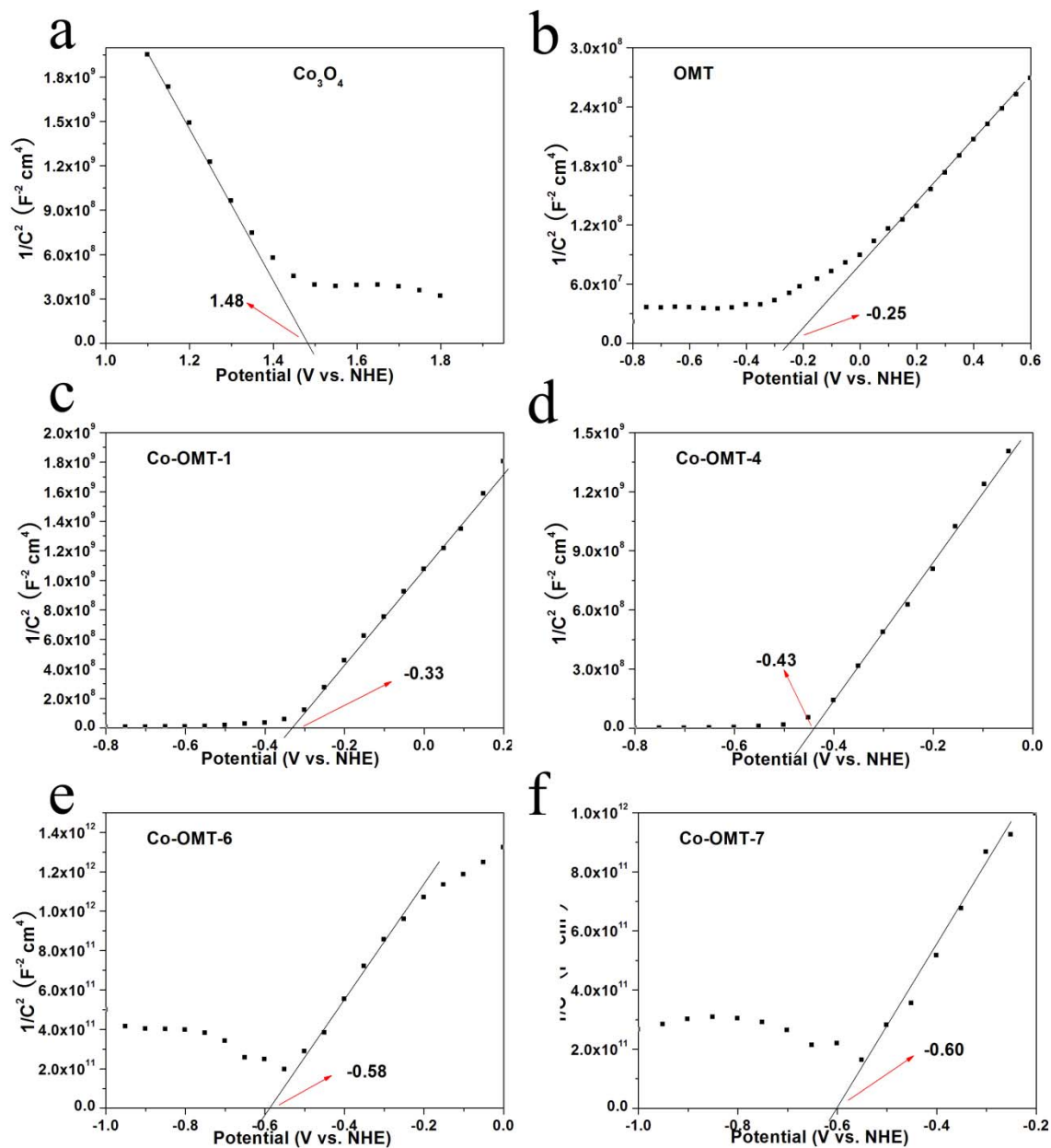


**Fig. S12** Mott-Schottky plots of samples: (a) OMT, (b) OMT, (c) Co-OMT-1, (d) Co-OMT-4, (e) Co-OMT-6, (f) Co-OMT-7.

## References

- R1. X. C. Wang , K. Maeda , A. Thomas , K. Takanabe , G. Xin , J. M. Carlsson , K. Domen, M. Antonietti, *Nat. Mater.*, 2009, **8**, 76–80.
- R2. S. E. Braslavsky, A. M. Braun, A. E. Cassano, A. V. Emeline, M. I. Litter, L. Palmisano, V. N. Parmon, N. Serpone, *Pure Appl. Chem.*, 2011, **83**, 931–1014.
- R3. S. N. Habisreutinger, L. Schmidt-Mende, J. K. Stolarczyk, *Angew. Chem. Int. Ed.*, 2013, **52**, 7372–7408.
- R4. S. Yan, H. Yu, N. Wang, Z. Li and Z. Zou, *Chem. Commun.*, 2012, **48**, 1048–1050.
- R5. J. Yu, J. Jin, B. Cheng and M. Jaroniec, *J. Mater. Chem. A*, 2014, **2**, 3407–3416.
- R6. T. Wang, X. Meng, P. Li, S. Ouyang, K. Chang, G. Liu, Z. Mei and J. Ye, *Nano Energy*, 2014, **9**, 50–60.
- R7. Q. Liu, Y. Zhou, J. Kou, X. Chen, Z. Tian, J. Gao, S. Yan and Z. G. Zou, *J. Am. Chem. Soc.*, 2010, **132**, 14385–14387.
- R8. J. Pan, X. Wu, L. Wang, G. Liu, G. Q. Lu and H. M. Cheng, *Chem. Commun.*, 2011, **47**, 8361–8363.
- R9. W. Jiao, L. Wang, G. Liu, G. Q. Lu and H. M. Cheng, *ACS Catal.*, 2012, **2**, 1854–1859.
- R10. H. Zhou, J. Guo, P. Li, T. X. Fan, D. Zhang and J. H. Ye, *Sci. Rep.*, 2013, **3**, 1667.
- R11. H. Zhou, P. Li, J. Guo, R. Yan, T. Fan, D. Zhang and J. Ye. *Nanoscales*, 2015, **7**, 113–120.
- R12. D. Kong, J. Ziang Y. Tan, F. Yang, J. Zeng and X. Zhang, *Appl. Surf. Sci.*, 2013, **277**, 105–110.

- R13. T. Ohno, T. Higo, N. Murakami, H. Saito, Q. Zhang, Y. Yang and T. Tsubota, *Appl. Catal. B*, 2014, **152–153**, 309–316.
- R14. M. Tahir, and N. S. Amin, *Appl. Catal. B*, 2015, **162**, 98–109.
- R15. Q. Li, L. Zong, C. Li and J. Yang. *Appl. Surf. Sci.*, 2014, **314**, 458–463.